Interactions of Alkali Metal Chlorides with Phosphatidylcholine Vesicles

Benjamin Klasczyk, Volker Knecht, Reinhard Lipowsky, and Rumiana Dimova*

Max Planck Institute of Colloids and Interfaces, Science Park Golm, 14424 Potsdam, Germany

Received September 10, 2010. Revised Manuscript Received November 8, 2010

We study the interaction of alkali metal chlorides with lipid vesicles made of palmitoyloleoylphosphatidylcholine (POPC). An elaborate set of techniques is used to investigate the binding process at physiological conditions. The alkali cation binding to POPC is characterized thermodynamically using isothermal titration calorimetry. The isotherms show that for all ions in the alkali group the binding process is endothermic, counterintuitively to what is expected for Coulomb interactions between the slightly negatively charged POPC liposomes and the cations. The process is entropy driven and presumably related to the liberation of water molecules from the hydration shells of the ions and the lipid headgroups. The measured molar enthalpies of the binding of the ions follows the Hofmeister series. The binding constants were also estimated, whereby lithium shows the strongest affinity to POPC membranes, followed by the rest of the ions according to the Hofmeister series. Cation adsorption increases the net surface potential of the vesicles as observed from electrophoretic mobility and zeta potential measurements. While lithium adsorption leads to slightly positive zeta potentials above a concentration of 100 mM, the adsorption of the rest of the ions mainly causes neutralization of the membrane. This is the first study characterizing the binding equilibrium of alkali metal chlorides to phosphatidylcholine membranes at physiological salt concentrations.

Introduction

Potassium and sodium ions are the first and second most abundant cations in the human body.[1] Thus, when studying cellular processes in biomimetic systems, they should be included in order to match the physiological conditions. Surprisingly, potassium is rarely employed and studied in the literature although it has similar physiological relevance to sodium. Whereas sodium is present at a higher concentration in the extracellular media of mammal organisms, potassium is located in comparable concentrations inside the cells (100−155 mM). Therefore, compared to sodium, the interaction of potassium with proteins and lipids is more important for their functionality inside the cell. While extracellular sodium has predominantly chloride as counterion, the intracellular cations, of which potassium is the most abundant, are not balanced equivalently by free anions. This phenomenon is also referred to as the anionic gap. The cellular electroneutrality inside the cells is established by the negatively charged proteins and the negatively charged lipids present mainly in the inner leaflet of the cell membrane and the organelle membranes.

The rest of the ions in the alkali metal series are also physiologically relevant. Lithium, rubidium, and cesium are present only at micromolar concentrations in the human body but are of medical importance as they can be curative or toxic depending on concentration. The medical applications relate to antidepressive, psychotherapeutical indication,[2,3] whereas a small aberrance from the curative concentration causes cardiac defects[4] or even death. It is still an issue of discussion whether such reactions are due to the fact that there is an influence on signal cascades in the biobalance of the biochemistry of cells.[5,6]

The interest toward understanding the effect of various types of ions on biological systems has triggered an outburst of studies in this field. On the basis of their propensity to precipitate proteins from aqueous solutions, in 1888 Hofmeister proposed a series which qualitatively arranged ions according to their efficiency; for extensive reviews see refs 7−9. For alkali cations, this series follows the order of increasing size of the bare ion (although some small deviations may occur depending on the measured physical quantity or the studied counterion[10]). The interaction of metal ions with membranes have also enticed significant interest initiated already 30 years ago. The focus was targeted on the precise characterization of ion binding to lipid bilayers and the corresponding change in the membrane surface potential. The majority of the work was based on measuring the interaction of multivalent cations with negatively charged membranes. The binding of monovalent cations to negatively charged bilayers was characterized by measurements on turbidity, electrophoretic mobility, and zeta potential of multilamellar or small unilamellar vesicles as well as investigated using deuterium nuclear magnetic resonance; see e.g. refs 11−15. The corresponding binding constants of the alkali cations with charged membranes were found to follow the Hofmeister series.[11]

Apart from the physiological relevance of the system negatively charged membranes−monovalent cations, the reason for the choice of studying ions and membranes which are oppositely charged was partially based on the fact that these interactions are stronger and thus easier to measure. However, there is a need for quantitative characterization of the binding stoichiometry and affinity of

*To whom correspondence should be addressed. E-mail: dimova@mpikg.mpg.de.

(1) Freitas, R. *Nanomedicine*; Landes Bioscience: Austin, TX, 1999.
(2) Aral, H.; Vecchio-Sadus, A. *Ecotoxicol. Environ. Saf.* **2008**, *70*, 349–356.
(3) Johnson, F. N. *Neurosci. Biobehav. Rev.* **1979**, *3*, 15–30.
(4) Melnikov, P.; Zanoni, L. Z. *Biol. Trace Elem. Res.* **2010**, *135*, 1–9.
(5) Williams, R.; Ryves, W.; Dalton, E.; Eickholt, B.; Shaltiel, G.; Agam, G.; Harwood, A. *Biochem. Soc. Trans.* **2004**, *32*, 799–802.
(6) Meltzer, H. L.; Taylor, R. M.; Platman, S. R.; Fieve, R. R. *Nature* **1969**, *223*, 321–322.

(7) Collins, M. W.; Washabaugh, K. D. *Q. Rev. Biophys.* **1985**, *18*, 323–422.
(8) Cacace, M. G.; Landau, E. M.; Ramsden, J. J. *Q. Rev. Biophys.* **1997**, *30*, 241–277.
(9) Kunz, W.; Henle, J.; Ninham, B. W. *Curr. Opin. Colloid Interface Sci.* **2004**, *9*, 19–37.
(10) Collins, K. D. *Methods* **2004**, *34*, 300–311.
(11) Eisenberg, M.; Gresalfi, T.; Riccio, T.; McLaughlin, S. *Biochem. J.* **1979**, *18*, 5213–5223.
(12) Roux, M.; Bloom, M. *Biochemistry* **1990**, *29*, 7077–7089.
(13) Ohki, S.; Ohshima, H. *Colloids Surf., B* **1999**, *14*, 27–45.
(14) Ruso, J. M.; Besada, L.; Martinez-Landeira, P.; Seoane, L.; Prieto, G.; Sarmiento, F. *J. Lipos. Res.* **2003**, *13*, 131–145.
(15) Claessens, M. M. A. E.; Leermakers, F. A. M.; Hoekstra, F. A.; Stuart, M. A. C. *J. Phys. Chem. B* **2007**, *111*, 7127–7132.

alkali ions to neutral lipids, which are more abundant but for which the interactions are much weaker and more difficult to measure, in particular, at low salt concentrations. With the technological advancement and improvement of many instrumental techniques, the limitation on measuring weak interactions is no longer present. Furthermore, with the enhanced development of computational power in the recent years, more precise data about membrane−ion interactions became accessible.[16,17]

The majority of previous experimental studies performed on neutral membranes explored high (molar, i.e., nonphysiological, or slightly submolar) concentrations of monovalent salts. X-ray scattering techniques and infrared spectroscopy showed that alkali chlorides influence the phase behavior of concentrated lipid bilayer systems.[18,19] At concentrations in the molar range, alkali ions were found to shift the main phase transition temperature of lipids by a few degrees.[20,21] The effect of the different ions follows the order in the Hofmeister series.[22] Monovalent cations were found to decrease the dipole potential of the lipid headgroups in phosphatidylcholine vesicles whereby the interaction was discussed in terms of free energies of hydration.[23] Recently, monovalent cations were also reported to affect the material properties of membranes. In particular, the bilayer bending rigidity decreases at high salt concentrations,[24,25] while the force needed to puncture supported bilayers increases with salt concentration.[26]

Molecular dynamics simulations were also employed to model the interactions between alkali metal chlorides and phosphatidylcholine (PC) bilayers. Two recent simulations on palmitoyloleoyl-phosphatidylcholine (POPC) bilayers in NaCl solutions have obtained a clearly defined Na^+ binding site within the PC headgroup region.[16,17] The effect of Li^+, Na^+, and K^+ at concentrations around 0.2 M was also compared.[27] Lithium was found to induce the strongest decrease in the area per lipid, and the maximal number of ions bound per lipid was estimated to be 0.28. Sodium and potassium showed weaker effects following the Hofmeister series. Sodium was also observed to bind more strongly to membranes than potassium whereas the chloride anions were found to mostly stay in the water phase.[16,17,28−30] Molecular dynamics simulations combined with fluorescence correlation spectroscopy found binding stoichiometry of one sodium cation to three POPC lipids and demonstrated that the ion binding leads to decreased lipid diffusion.[17] The bending moduli of the membrane leaflets were also determined from studies on an asymmetric PC bilayer facing sodium chloride on one side and potassium chloride on the other. The leaflet facing sodium was found to be stiffer than the one facing potassium.[31] Because of the small sizes of the simulation boxes, mainly high ionic concentrations (between 0.2 and 1 M) were accessible in these studies.

Here, we focus on the interaction of neutral phosphatidylcholine bilayers with monovalent alkali chlorides at low and physiological concentrations. A detailed characterization of the adsorption of ions onto membranes is highly desirable in order to understand the behavior of proteins whose functions and kinetics are dependent on the local ion concentration. One example is provided by ion pumps such as the Na^+ and K^+-ATPase, for which the cations may not only affect the protein structure and stability.[7] One can easily imagine that the protein function and performance depend on the local ion concentration in the immediate vicinity of the membrane. The stability and binding of proteins to membranes also depend on ion binding.[19] This motivated us to characterize in detail the thermodynamic parameters describing the binding of the ions to the membrane but also the ion distribution in the bilayer vicinity. The binding of the ions is described by the equilibrium binding constant and the molar enthalpy of interaction, while information on the ion distribution can be deduced from the zeta potential of vesicles in solutions of different salt concentrations.

To the best of our knowledge, we report here the first systematic study comparing all alkali metal chlorides according to their binding strength to PC membranes. The majority of the data are collected with two experimental methods: highly sensitive isothermal titration calorimetry (ITC) and zeta potential measurements. Dynamic light scattering and differential scanning calorimetry were also employed. We quantitatively characterize the interaction of alkali metal ions with neutral POPC membranes and discuss it in relation to the Hofmeister series. While ITC provides us with the thermodynamic characterization of the strength and stoichiometry of the ion−lipid binding, the zeta potential measurements provide information about the ion concentration in the immediate vicinity of the membrane.

Experimental Section

Materials. 1-Palmitoyl-2-oleoyl-*sn*-glycero-3-phosphatidyl-choline (POPC) and 1,2-dimyristoyl-*sn*-glycero-3-phosphocholine (DMPC) were obtained from Avanti Polar Lipids Inc. (Alabaster, AL) and used as received. Lithium chloride (LiCl), sodium chloride (NaCl), potassium chloride (KCl), and rubidium chloride (RbCl) were purchased from Sigma-Aldrich (Steinheim, Germany). Cesium chloride (CsCl) was purchased from Merck (Darmstadt, Germany).

Alkali chloride solutions in the concentration range from 10 to 500 mM were prepared freshly before use, and their osmolarities were measured with cryoscopic osmometer Osmomat 030 (Gonotec, Berlin, Germany). The ionic solutions were buffered using 15 mM HEPES and adjusted to pH 7.0 with 1 M KOH (both obtained from Sigma-Aldrich). This adjustment leads to the presence of less than about 2 mM potassium cations in the solutions, but this concentration does not change the measured observables beyond the standard deviation.

Vesicle Preparation. For the vesicle preparations, we used POPC dissolved in chloroform. For the differential scanning calorimetry measurements we also used DMPC. The solutions were pipetted into glass flasks and dried under nitrogen flow. The open flasks were placed under vacuum for 1 h to remove traces of the organic solvent. Then, the lipids were hydrated by adding the respective salt or buffer solution to a final lipid concentration of 2 mM. The flasks were shaken for several minutes at room temperature.

Large unilamellar vesicles (LUVs) were prepared by extruding the obtained lipid dispersions with LiposoFast pneumatic extruder (Avestin, Otawa, Canada) successively through polycarbonate membranes (Avestin Europe, Germany) from 400, to 200, and to 100 nm pore diameter. The lipid dispersion was extruded through

(16) Pandit, S. A.; Bostick, D.; Berkowitz, M. L. *Biophys. J.* **2003**, *84*, 3743–3750.

(17) Böckmann, R. A.; Hac, A.; Heimburg, T.; Grubmuller, H. *Biophys. J.* **2003**, *85*, 1647–1655.

(18) Rappolt, M.; Pressl, K.; Pabst, G.; Laggner, P. *Biochim. Biophys. Acta, Biomembr.* **1998**, *1372*, 389–393.

(19) Binder, H.; Zschörnig, O. *Chem. Phys. Lipids* **2002**, *115*, 39–61.

(20) Cunningham, B.; Shimotake, J. E.; Tamura-Lis, W.; Mastran, T.; Kwok, W. M.; Kauffman, J. W.; Lis, L. J. *Chem. Phys. Lipids* **1986**, *39*, 135–143.

(21) Bartucci, R.; Sportelli, L. *Colloid Polym. Sci.* **1993**, *271*, 262–267.

(22) Koynova, R.; Brankov, J.; Tenchov, B. *Eur. Biophys. J.* **1997**, *25*, 261–274.

(23) Clarke, R. J.; Lüpfert, C. *Biophys. J.* **1999**, *76*, 2614–2624.

(24) Pabst, G.; Hodzic, A.; Strancar, J.; Danner, S.; Rappolt, M.; Laggner, P. *Biophys. J.* **2007**, *93*, 2688–2696.

(25) Bouvrais, H.; Méléard, P.; Pott, T.; Ipsen, J. H. *Biophys. J.* **2009**, *96*, 161.

(26) Garcia-Manyes, S.; Oncins, G.; Sanz, F. *Biophys. J.* **2005**, *89*, 1812–1826.

(27) Cordomi, A.; Edholm, O.; Perez, J. J. *J. Phys. Chem. B* **2008**, *112*, 1397–1408.

(28) Gurtovenko, A. A.; Vattulainen, I. *J. Phys. Chem. B* **2008**, *112*, 1953.

(29) Vacha, R.; Siu, S. W. I.; Petrov, M.; Bockmann, R. A.; Barucha-Kraszewska, J.; Jurkiewicz, P.; Hof, M.; Berkowitz, M. L.; Jungwirth, P. *J. Phys. Chem. A* **2009**, *113*, 7235–7243.

(30) Vacha, R.; Berkowitz, M. L.; Jungwirth, P. *Biophys. J.* **2009**, *96*, 4493–4501.

(31) Lee, S.; Song, Y.; Baker, N. *Biophys. J.* **2008**, *94*, 3565–3576.

the 400 and 200 nm pore membranes 20 times and through the 100 nm pore membrane 40 times. The final step involved degassing of the vesicle solutions for 8 min in vacuum chamber ThermoVac (MicroCal; Northhampton, MA). This step is important before performing all measurements as gas bubbles introduced in the sample during the extrusion lead to artifacts.

Zeta Potential and Dynamic Light Scattering Measurements. Electrophoretic mobilities and size distribution of the extruded vesicles were determined at 27 °C with a Zetasizer Nano ZS (Malvern Instruments, Worcestershire, UK) operating with a 4 mW HeNe laser (632.8 nm), a detector positioned at the scattering angle of 173°, and a temperature-control jacket for the cuvette. The cuvette was sealed to avoid evaporation and left for 3 min in the instrument for temperature equilibration. Five dynamic light scattering (DLS) measurements consisting of up to 15 consecutive runs with duration of 10 s were performed for each sample. Dynamic correlation functions were fitted by a second-order cumulant method to obtain the size distributions. For the zeta potential measurements, the samples with volume 0.75 mL, 2 mM lipid concentration, and varied salts were loaded in folded capillary cells with integral gold electrodes. More than ten measurements, each consisting of 100−500 runs with duration of 3 s, were performed for every sample at 27 °C. For each concentration, at least two independent preparations were explored.

The measured electrophoretic mobility μ_e provides information about the effective charge Q_{eff} of the vesicles experiencing hydrodynamic friction during the measurement:

$$\mu_e = \frac{1}{6\pi\eta}\frac{Q_{eff}}{R_{eff}} \tag{1}$$

where R_{eff} is the effective radius of the vesicle including the Stern layer and η is the viscosity of the aqueous solution. The electrophoretic mobility can be converted to zeta potential, ζ, using a model described by the Smoluchowski and Hückel equation[32]

$$\zeta = \frac{3\mu_e\eta}{2\varepsilon_0\varepsilon f(\kappa R)} \tag{2}$$

where ε_0 and ε are the permittivity of free space and the relative permittivity of the medium, respectively. The Henry function,[32] $f(\kappa R)$, for a nonconducting sphere depends on the radius R of the vesicle and the inverse Debye length $\kappa = (e^2 2C_{ion}/\varepsilon_0\varepsilon k_B T)^{1/2}$ for monovalent electrolytes, where e is the elementary charge, C_{ion} is the electrolyte concentration, k_B is the Boltzmann constant, and T is the temperature:

$$f(\kappa R) = f(C_{ion}, R)$$
$$\approx \begin{cases} 1 & \text{for } \kappa R < 1 \\ \frac{1}{6}\log(\kappa R)+1 & \text{for } 1 < \kappa R < 1000 \\ 1.5 & \text{for } \kappa R > 1000 \end{cases} \tag{3}$$

For a large particle with a relatively thin double layer, $\kappa R > 1000$ and the Smoluchowski−Hückel equation (eq 2) loses the prefactor 3/2. In the concentration regime explored here, from 0 to 500 mM, the prefactor varies in a certain range as shown in Figure 1. This dependence was taken into account in the analysis of the zeta potential results.

Isothermal Titration Calorimetry. The ITC measurements were performed with a VP-ITC microcalorimeter from MicroCal (Northhampton, MA). The instrument has a pair of identical coin-shaped cells enclosed in an adiabatic jacket, a reference cell, and a working cell. The working cell has a volume of 1.442 mL, and before the measurement it was filled with the sample solution of POPC LUVs (2 mM) in HEPES buffer without ions. The reference cell was filled with a HEPES buffer only. The alkali metal chloride dissolved in HEPES solution in a concentration of 500 mM (titrant) was injected stepwise in 10 μL aliquots into the working cell via a syringe with total volume of 288 μL. The time
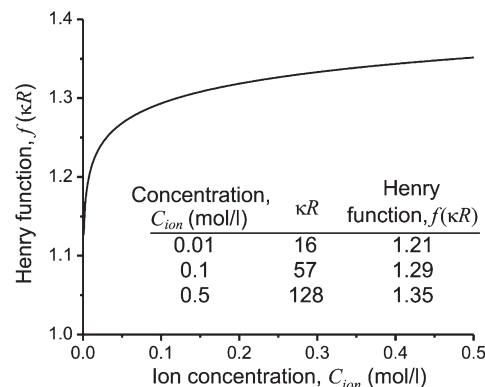

Figure 1. Henry function as a correction factor of the model for the zeta potential (eq 2) calculated for vesicle radius $R = 56$ nm as measured with DLS. The table inset gives examples for $f(\kappa R)$ for certain salt concentrations.

Concentration, C_{ion} (mol/l)	κR	Henry function, $f(\kappa R)$
0.01	16	1.21
0.1	57	1.29
0.5	128	1.35

interval between two consecutive injections was 200 s, of which the injection itself takes 20 s. The first injection was set to a volume of 2 μL and was ignored in the data analysis due to dilution occurring during the equilibration stage before the measurement. The sample was constantly stirred with the syringe tip at a stirring rate of 310 rpm. The measurements were performed at constant temperature of 27 °C. Each injection produced a characteristic peak in the measured heat flow arising from the released or absorbed heat corresponding to downward- or upward-pointing peak, respectively. In the analysis, a baseline was subtracted from the data, corresponding to the signal between consecutive injections when no change in the heat flow was detected. Subsequent integration of the peak signal over time provided the heat per injection. The data analysis was performed using the Origin software provided by MicroCal. The binding heat per injection was evaluated after subtracting the following reference measurements from the ion-into-lipid titrations: titration of alkali metal chloride HEPES solutions into pure HEPES solution without lipids and dilution of the vesicles titrated with buffer. These dilution corrections, however, subtract twice the heat associated with mechanical work associated with the actual injection, which can be estimated from injecting HEPES into HEPES solution. Therefore, the data were corrected additionally by adding this heat. The dilution measurements of injecting pure buffer into buffered vesicle solution produce much weaker signal than the heat of salt dilution as determined from injecting alkali metal chlorides into HEPES buffer. The standard error was determined by averaging over three experiments.

After subtracting the heats of dilution, the ITC data were used to determine the enthalpy associated with the binding of alkali cations to the POPC vesicles. The change in heat δq per injection is proportional to the molar enthalpy, ΔH, characterizing the interaction

$$\delta q = \delta n_{lip}^b \Delta H \tag{4}$$

where $\delta n_{lip}^b = \delta C_{lip}^b V_{cell}$ is the change in the moles of lipid bound by the cations after the injection. Here δC_{lip}^b is the change in the concentration of the bound lipid, and V_{cell} is the current volume of the chamber. Assuming a simple partition equilibrium of 1:1 ion to lipid complex formation,[33,34] the apparent binding constant K can be defined as

$$K \approx \frac{C_{lip}^b}{C_{ion}(C_{lip} - C_{lip}^b)} \tag{5}$$

where C_{lip} is the total concentration of lipids available for binding. The difference $C_{lip} - C_{lip}^b$ represents the concentration of free, unbound lipids. Above, we have assumed that the concentration of the unbound ions is approximately equal to the total ion

(32) Hunter, R. *Zeta Potential in Colloid Science*; Academic Press: New York, 1981.

(33) Heerklotz, H.; Seelig, J. *Biophys. J.* **2000**, *78*, 2435–2440.
(34) Huster, D.; Arnold, K.; Gawrisch, K. *Biophys. J.* **2000**, *78*, 3011–3018.

concentration C_{ion}. We express the concentration of the bound lipid using eq 5 and insert the derivative with respect to the total electrolyte concentration C_{ion} into eq 4, which leads to

$$\delta q = \delta C_{ion} \frac{KC_{lip}}{(1+KC_{ion})^2} V_{cell} \Delta H \qquad (6)$$

Here, the change in the total ion concentration δC_{ion}, the total ion concentration C_{ion}, and the current volume V_{cell} of the measurement chamber are known from the experiments. For the lipid concentration, only the outer bilayer leaflet of the lipid vesicle is considered, corresponding to 55% of the total lipid concentration (calculated for 56 nm vesicle radius as measured with DLS; see Results and Discussion section). Fitting the data with eq 6, one obtains the apparent binding constant K and the reaction molar enthalpy ΔH.

Differential Scanning Calorimetry. Differential scanning calorimetry (DSC) measurements were performed with a Micro-Cal VP-DSC scanning calorimeter (MicroCal, Inc., Northhampton, MA). The heating and cooling rates were set to 20 K/h, and the measurements were performed in the temperature interval from 4 to 60 °C. The lipid concentration was 2 mM. The reproducibility of the DSC experiments was checked by four consecutive scans of each sample.

Results and Discussion

Membrane Surface Charge. The LUVs prepared in solutions with different electrolyte concentration had an average radius of $R = 56.1 \pm 2.4$ nm irrespective of the type of the alkali metal chloride. The electrolyte concentration was varied in the range from 10 to 500 mM. In the absence of salt, the vesicles have a weak negative zeta potential even though the phosphatidylcholine group is zwitterionic and thus uncharged at neutral pH. The negative zeta potential has been interpreted in terms of the orientation of the hydration layers[35] and lipid headgroups,[36] water polarization,[37] as well as arising from impurities.[38]

The results for the electrophoretic mobility measured at different salt concentrations are summarized in Figure 2A. The effective charge on the vesicles, Q_{eff}, can be estimated using eq 1. For the effective vesicle size R_{eff} one can take the approximate vesicle radius, R, as measured with DLS, having in mind that the Stern layer or the shear plane are located a few water layers away, which is a relatively small distance compared to the vesicle diameter of the order of 100 nm. With increasing concentration, the net value of the surface charge increases for all ions; see right axis in Figure 2A. Assuming that the competition between chloride and alkali ions binding to the membrane is in favor of the cations as suggested by earlier studies,[16,17,29,30,39] this behavior directly implies adsorption of the alkali cations to the PC membrane. Above a concentration of around 150 mM, the effective charge exhibits a plateau, suggesting saturation of the ion−membrane interactions. Note that this occurs at ratios of lipid to ion bulk concentrations smaller than 1:50.

Although the zeta potential does not directly represent the membrane surface charge, but the charge at the shear plane (where the Stern layer and the diffuse layer meet), it is believed to provide a good approximation of the surface potential for low and moderate electrolyte concentrations up to 0.1 M.[32,40] At higher concentrations, however, since the experimentally measured standard deviations are relatively large, the uncertainty in the interpolation
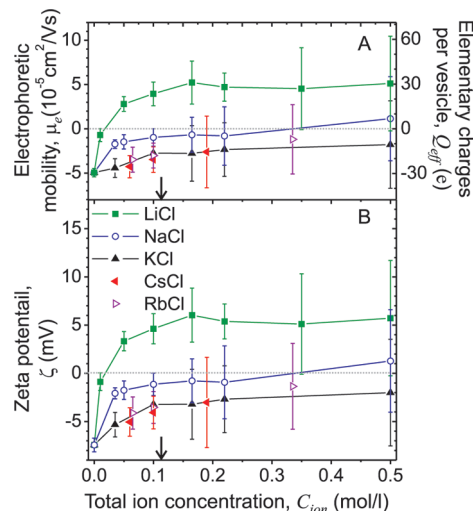

Figure 2. Electrophoretic mobility (A) and zeta potential of POPC LUVs (B). In (A), right axis, we also give the corresponding elementary charges per vesicle (see eq 1). The data were collected for vesicles with total lipid concentration of 2 mM prepared in solutions of alkali metal chlorides. The error bars represent standard deviations. The arrows approximately indicate the final concentration of alkali metal chlorides at the end of the ITC experiments.

formula (eq 2) is not the limiting factor. Using this expression, we estimated the zeta potential of the vesicles in the presence of the different alkali salt solutions (see Figure 2B). At high electrolyte concentrations, i.e., high conductivities, the voltage applied during the electrophoretic mobility measurements should be lowered to avoid electrolysis at the electrodes. This decreases the measurement resolution (compare the error bars). In ref 14, zeta potential measurements performed on essentially the same instrument were reported on charged lipid vesicles at salt concentrations up to 1 M and used to distinguish the effect of sodium, potassium, and cesium. In contrast, for such high conductivities, we were not able to resolve significant differences in the electrophoretic mobility for these ions considering the measurement error (see Figure 2). Below physiological concentrations of around 150 mM, the standard deviation is relatively small, and it is possible to clearly distinguish the effects of lithium, sodium, and potassium chlorides. Rubidium and cesium chlorides do not show significant differences from the data obtained for potassium chloride. Above 150 mM, only LiCl can be distinguished from the rest of the alkali metal chlorides. Lithium ions show the strongest affinity to POPC membranes, shifting the vesicle zeta potential to even slightly positive values considering the error bars. At saturation levels, the effective charge density of 60 lithium ions at the membrane corresponds to approximately one ion per area of 660 nm^2. Note that 60 lithium ions are necessary to change the charge of the vesicles from −30 to +30 elementary charges per vesicle. The respective interionic distance is much larger than the Debye screening length at these concentrations.

To summarize, the zeta potential results indicate adsorption of alkali metal cations to zwitterionic POPC membranes following the order of the Hofmeister series:

$$\zeta(Li) > \zeta(Na) > \zeta(K) \sim \zeta(Rb) \sim \zeta(Cs)$$

In principle, the zeta potential may be used for estimating an equilibrium constant characterizing the process either using the Stern isotherm and the Gouy−Chapman theory,[14] the theory of the electrical double layer,[41] or provided additional data on the

(35) Egawa, H.; Furusawa, K. *Langmuir* **1999**, *15*, 1660–1666.
(36) Makino, K.; Yamada, T.; Kimura, M.; Oka, T.; Ohshima, H.; Kondo, T. *Biophys. Chem.* **1991**, *41*, 175–183.
(37) Knecht, V.; Levine, Z. A.; Vernier, P. T. *J. Colloid Interface Sci.* **2010**, doi: 10.1016/j.jcis.2010.07.002.
(38) Pincet, F.; Cribier, S.; Perez, E. *Eur. Phys. J. B* **1999**, *11*, 127–130.
(39) Clarke, R. J.; Lupfert, C. *Biophys. J.* **1999**, *76*, 2614–2624.
(40) Lyklema, J. *J. Colloid Interface Sci.* **1977**, *58*, 242–250.

(41) Tatulian, S. A. *Eur. J. Biochem.* **1987**, *170*, 413–420.
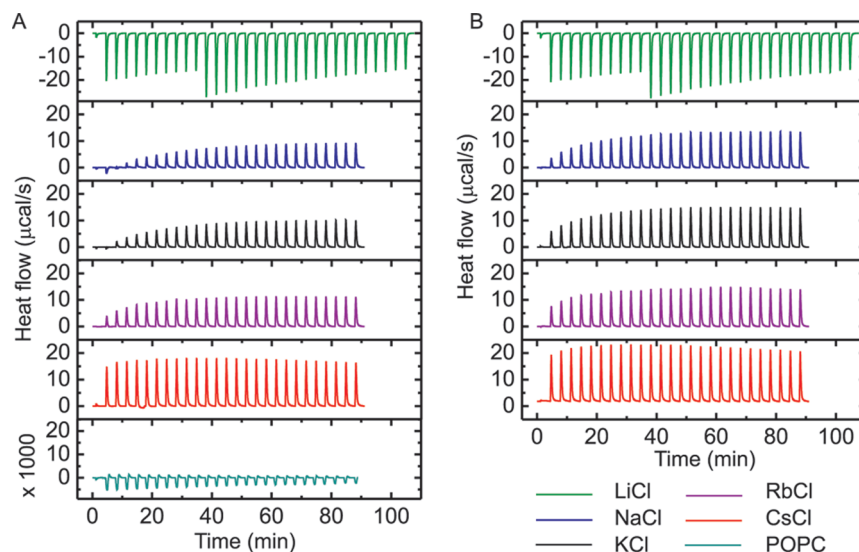
Figure 3. Raw data from ITC measurements of the heats of dilution or reference measurements (A) and binding titration (B). The heat flows were measured for injecting 10 μL aliquots of buffered alkali chlorides (500 mM) in HEPES solutions (A) or in 2 mM POPC solution (B). Because of the limited power range of the calorimeter, the first 10 LiCl injections were reduced to 5 μL. This was accounted for in the data analysis. The last graph in panel A shows the heat flow from injecting 10 μL aliquots HEPES buffer into 2 mM POPC buffered solution; note that the signal is very weak, and the axis was multiplied by 1000.

area per lipid are available from X-rays and NMR experiments as proposed in ref 34. However, the relatively large error in our data does not allow for distinguishing the specific effects of potassium, rubidium, and cesium. We also emphasize that the zeta potential characterizes the amount of ions located in the membrane vicinity and not necessarily the amount of bound ions. Evaluating the latter is possible from the ITC data as discussed in the next section.

Ion Binding to POPC Membranes. Compared to the zeta potential measurements, which furnish information about the surface concentration of ions close to the membrane, the ITC measurements provide a way to evaluate the actual binding of the ions to the membrane characterized by equilibrium constants and reaction enthalpies.

ITC experiments were done titrating buffered solutions of alkali metal chlorides with a concentration of 500 mM into 2 mM LUV suspensions buffered in HEPES. The final ion concentration in the measuring cell was about 100 mM (in one additional experiment for each alkali chloride, we explored concentrations up to 150 mM). During the titration measurements, the vesicle radii decreased by about 5 nm (to final average radius of $\simeq$51 nm as measured with DLS) because of osmotic shrinking. The heat contributions associated with this process are negligible.[42]

Reference measurements (see subsection Isothermal Titration Calorimetry in the Experimental Section) were also performed to evaluate the heat associated with diluting the chlorides into buffer and the heat due to injecting buffer into the vesicle solution. Figure 3 shows calorimetric traces of the experiments and the corresponding reference measurements (for the integrated heats per injection see the Supporting Information). The difference between the ion-to-lipid titrations (Figure 3B) and the reference measurements (Figure 3A) is small, indicating a relatively weak signal from binding of the ions to the membrane. Except for lithium chloride, the ion dilution and the ion-to-vesicle titrations produce endothermic signals.

The results from the ion dilution reference measurements (Figure 3A) are interesting on their own and were investigated
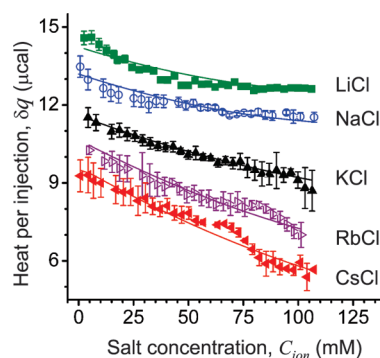

Figure 4. Heat release δq arising from binding of alkali ions to the membrane. The error bars represent standard error as estimated from repeating the measurements. The solid curves are fits according to the partition model, eq 6, introduced in the section Isothermal Titration Calorimetry.

in detail in previous studies.[43,44] Here, we only provide estimates for the molar enthalpies of salt dilution, ΔH_{dil}, which can be obtained from extrapolation of the integrated heats of dilution to zero ion concentration. For LiCl, NaCl, KCl, CsCl, and RbCl dilution buffered in HEPES at pH 7.0, for ΔH_{dil} we obtain approximately -70, -14, -4, 16, and 60 kcal/mol, respectively. The values follow the order in the Hofmeister series; i.e., ΔH_{dil} increases with the ion size.

The binding heat per injection δq corrected for dilution effects as explained in the subsection Isothermal Titration Calorimetry is plotted in Figure 4 as a function of the electrolyte concentration, which increases with the number of injections. The binding of the ions to the membrane produces positive values for δq for all alkali ions, indicating endothermic binding processes. Note that even though the binding measurement with lithium chloride in Figure 3B is exothermic, subtracting the heat per injection of the respective reference measurement in Figure 3A yields positive (endothermic) values for the binding heat per injection δq.

(42) Nebel, S.; Ganz, P.; Seelig, J. *Biochem. J.* **1997**, *36*, 2853–2859.
(43) Kroener, J. Ph.D. Thesis, University of Regensburg, 1997.
(44) Sinn, C. G. Ph.D. Thesis, University of Potsdam, 2004.

Considering that the total lipid concentration in the sample is less than 2 mM throughout the ITC titration, the data misleadingly suggest that the binding process continues even beyond 1:1 ion:lipid molar stoichiometry of the bulk salt and lipid concentrations. This is also observed in the electrophoretic mobility measurements and in general implies that the lipid membrane can bind more ions than it possesses lipid molecules. Let us however emphasize that the amount of bound ions is only a small fraction of the total amount of ions in the solution.

The data for δq can be fitted using eq 6, from which we obtain both the binding constant K and the molar enthalpy of the process ΔH as shown in Figure 4. Because of the relatively large error in the data, we did not try to fit the data with more sophisticated models. In our analysis, we assume that the competition between chloride and alkali ions binding to the membrane is in favor of the cations as suggested by earlier studies.[16,17,29,30,39] To ensure a more robust determination of K and ΔH, the separate measurements for each alkali chloride were fitted simultaneously irrespective of the explored concentration range. (Note that if three measurements are fitted simultaneously, the number of fitting parameters per curve is less than one, and the fitting parameters are thus determined more precisely.) The obtained values for the apparent binding constant K are given in Table 1. The order of magnitude of the estimated values of K indicates that the concentration of free ions is indeed approximately equal to that of the total ion concentration, suggesting self-consistency of the model (see eq 5 and the assumption following it).

The value of the apparent binding constant K depends on the explored range of salt concentrations, i.e., the ionic strength of the solution. The definition of K ignores the role of electrostatic attraction between the slightly negatively charged POPC vesicles and the cations. However, because the membrane is only weakly charged and the explored range of salt concentrations in the different measurements identical, the apparent binding constant would not differ significantly from the so-called intrinsic binding constant. The latter takes into account the enhanced concentration of ions close to the membrane. Larger discrepancies between to the two constants will be observed for vesicles made of negatively charged lipids and measurements performed in different salt concentration ranges. Here we report the data for the apparent binding constant simply because they are easier to consider for the specific experimental conditions and can be calculated directly from the binding isotherm without further knowledge about the ion distribution (see e.g. ref 45). The results are summarized in Table 1.

Even though the errors are relatively large to distinguish the effect of some of the neighboring cations in the alkali series, the trend exhibited by the average values of the obtained molar enthalpies and binding constants clearly follow the Hofmeister series. They decrease with the size of the bare cation from lithium to cesium. The binding constants measured earlier for the interactions of these ions with negatively charged phosphatidylserine membranes were also found to follow this trend.[11] Indeed, they are of the same order of magnitude, suggesting that the affinity of alkali cations to charged and neutral membranes is similar. Likewise, the affinity of calcium ions to these two membrane types was also found previously not to differ significantly.[46]

The values we obtained for the binding constants for sodium correspond well to data reported in the literature; for the rest of the alkali cations, such data are not available. Molecular dynamics

Table 1. Thermodynamic Parameters Characterizing the Binding of Alkali Metal Cations to POPC Vesicles (Standard Errors Are Also Given)

alkali cation	apparent binding constant, K [l/mol]	molar enthalpy, ΔH [kcal/mol]	Gibbs free energy, ΔG [kcal/mol]	entropic contribution, $T\Delta S$ [kcal/mol]
Li	1.37 ± 0.06	2.39 ± 0.09	-2.58 ± 0.03	4.97 ± 0.09
Na	1.25 ± 0.05	2.33 ± 0.09	-2.53 ± 0.02	4.86 ± 0.09
K	1.17 ± 0.13	2.13 ± 0.23	-2.49 ± 0.07	4.62 ± 0.24
Rb	1.14 ± 0.28	1.75 ± 0.40	-2.47 ± 0.15	4.22 ± 0.43
Cs	1.10 ± 0.14	1.67 ± 0.19	-2.45 ± 0.08	4.12 ± 0.20

simulations on dipalmytoylphosphatidylcholine in the fluid phase provide binding constants in the range between 0.15 and $0.61 \ M^{-1}$.[16] In contrast to our experimental system, these simulations were performed for lipid bilayers in the absence of buffering agents which might influence the binding equilibrium. Zeta potential measurements on egg phosphatidylcholine multilamellar liposomes suggest the value $0.15 \pm 0.1 \ M^{-1}$ for the intrinsic binding constant of sodium.[41] These somewhat lower values for the binding constant could arise because in these latter studies a mixture of several lipid species has been used. Note also that depending on the specific conditions, i.e., composition of buffer, pH, presence of competing ions like calcium, the value of the binding constant may change. Furthermore, a careful comparison of the available data requires considering whether the measured binding constants are the intrinsic or apparent ones, which is important if different ranges of salt concentrations are explored in the studies.

The molar enthalpies measured for all alkali metal cations adsorbing to the membrane are positive (endothermic), indicating that this interaction is entropically driven. Intuitively, one would have expected predominant Coulombic interactions between the positively charged cations and the slightly negatively charged liposomes yielding exothermic signal. However, our results suggest that the endothermic character of the binding process can be understood in terms of entropy gain. The binding of the cations to the lipids perturbs the hydration shells of both binding partners and leads to the liberation of water molecules.[47] Similar behavior was observed for calcium ions binding to oppositely charged membranes[46] and polymers.[48]

To quantitatively evaluate the entropic contribution involved in the binding of the alkali cations to the membrane, we first deduce the Gibbs free energy of the process, ΔG. The latter is estimated from the binding constant following the relation $\Delta G = -RT \ln(55.5K)$ (where ΔG is defined for standard state of mole fractions and the factor 55.5 introduces the concentration of water). The obtained values are given in Table 1. The entropy gain can then be estimated from the Gibbs free energy via $T\Delta S = \Delta H - \Delta G$. For all alkali chlorides the entropic contribution is larger than the enthalpic one (see Table 1). Presumably, the entropy gain arises from the release of water molecules. A naive estimate for the number of released water molecules can be made from the change in the internal energy. The latter is approximately equal to the enthalpy change ΔH if we assume that both the density and the pair distribution functions of the bound water molecules are roughly equal to those of the liberated water molecules. Then, from the equipartition theorem, it follows that $\Delta H \simeq n(f/2)k_{B}T - (3/2)k_{B}T$. Here, n is the number of released

(45) Wenk, M. R.; Seelig, J. *Biochemistry* **1998**, *37*, 3909–3916.
(46) Sinn, C. G.; Antonietti, M.; Dimova, R. *Colloids Surf., A* **2006**, *282*, 410–419.

(47) Dimova, R.; Lipowsky, R.; Mastai, Y.; Antonietti, M. *Langmuir* **2003**, *19*, 6097–6103.
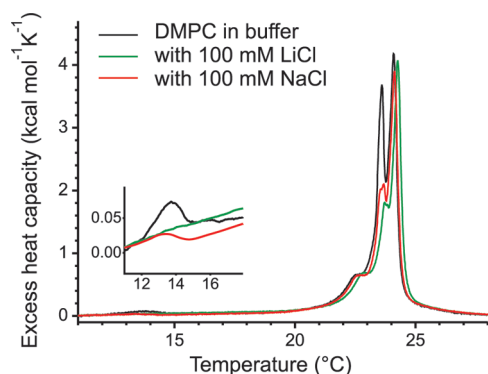(48) Sinn, C. G.; Dimova, R.; Antonietti, M. *Macromolecules* **2004**, *37*, 3444–3450.

Figure 5. Heat capacity profiles of the main transition of DMPC LUVs extruded in HEPES buffer in the absence of salt (black curve) and in the presence of 100 mM LiCl (green curve) or 100 mM NaCl (red curve) in the vesicle exterior. The pretransition occurring around 14 °C is suppressed in the presence of the salts. The inset shows an enlarged view of the temperature region around the pretransition.

water molecules and f is the number of classical degrees of freedom. When released, a single water molecule gains three translational and up to three rotational degrees of freedom, i.e., $3 \leq f \leq 6$. Using $f = 3$, we estimate that between 2 and 4 water molecules are released from the lipid and the cation hydration shells upon the binding of one cation. The number decreases with increasing the size of the bare cation following the Hofmeister series. A naive explanation for this observation could be that the hydration number for the larger ions is smaller; thus, less water molecules can be liberated.

To compare the heat contributions measured with ITC with those due to possible changes in the phase state of the lipid, we conducted DSC measurements. Calorimetry data can provide evidence for the hydration/dehydration effects of the lipids upon ion binding. Because of the limited temperature range of the DSC device and because DSC experiments on vesicle solutions are restricted to temperatures above the freezing point of water, the experiments were performed using DMPC instead of POPC. The main phase transition temperature of DMPC is about 23 °C,[49] whereas the transition temperature of POPC is approximately −3 °C.[50] Even though these two lipids are structurally different, they have identical headgroups, which are most essential for ion binding. The excess heat capacities of DMPC LUVs solutions in HEPES buffer in the absence and presence of salt are shown in Figure 5. Only LiCl and NaCl were explored since these salts showed the most significant effect in the zeta potential and ITC measurements.

In salt-free solution, the vesicle suspension shows an endothermic phase transition. Splitting of the main transition peak is observed, which is characteristic for samples with extruded vesicles.[51] Presumably it is due to structural transitions in the vesicles that might be associated with loss of correlation among the lipid headgroups and trans−gauche isomerization in the chains. A weak peak for the pretransition of DMPC (formation of the ripple phase) around 14 °C is also detected. The integral area of the profile yields for the melting enthalpy $\Delta H_{melt} \approx 4.95 \pm 0.13$ kcal/mol.

We also explored vesicle samples with two electrolyte solutions, namely LiCl and NaCl at concentration of 100 mM, which approximately corresponds to the concentration at the end of the

ITC measurements. The salt solutions were added to the extruded vesicle suspensions mimicking the conditions in the ITC cell at this concentration. The melting enthalpy of the transition ΔH_{melt} drops down to $\approx 4.59 \pm 0.10$ kcal/mol for both salts. Since we do not observe significant difference in the behavior of the salts in this respect, we conclude that the differences in the molar enthalpy of the ion−membrane interactions are not due to changes in the phase state of the lipid.

Previous work has demonstrated a shift in the gel-to-fluid phase transition temperatures in POPC bilayer stacks to higher temperatures and broadening of the overall calorimetric profile.[17] An even stronger increase was observed in the main phase transition temperature of charged lipids in the presence of salt.[52] Here, we observe only a mild shift in the calorimetric traces toward higher temperature in the presence of the salt solutions, which is better expressed in the LiCl trace. The weak shifts in the heat capacity profiles in the presence of the salts suggest ion-induced structural changes arising from rearrangement either in the hydrocarbon chain packing or of the polar headgroup packing, e.g., changes of the hydration shell. Molecular dynamics simulations have shown that Li$^+$ and Na$^+$ reduce the area per lipid, hence increasing the ordering of the lipid tails, which may be related to the slight increase in the main transition temperature.[17,27] Since the shifts observed in Figure 5 are to higher temperatures, the packing of the lipids in the presence of the ions is energetically more stable, and the interaction with the sodium ions favors the ordered low-temperature phase. The DSC data indicate that this stabilization is similar for LiCl and NaCl. The shape of the main peak is also changed by the presence of the ions, whereby the first part of the peak is suppressed. On a speculative basis one can presumably interpret this as a consequence of loss of correlation among the lipid headgroups. Yet another interesting observation concerns the lipid pretransition. It seems to be completely suppressed in the presence of the salts. Indeed, this pretransition has been previously discussed as a consequence of coupling of structural changes and chain melting transitions.[53] In particular, the occurrence of the ripples has been considered as formation of defects of fluid molecules. Apparently, our measurements suggest that these defects are less expressed in the presence of lithium and sodium chlorides, supporting furthermore the stabilizing effect of these salts.

Conclusion

Knowledge of the physicochemical properties of lipid bilayers is crucial for the understanding of their functions and behavior. One of the main physiological roles of the plasma membrane is to ensure compartmentalization of electrolyte solutions in and out of the cell. Therefore, it is of great importance to understand how salt solutions affect the membrane. We used a combination of experimental techniques to address this problem. The ITC measurements show that binding of ions to phosphocholine bilayers occurs spontaneously but is an endothermic process, and therefore, entropy driven. The gain in entropy presumably arises from the release of several water molecules from the hydration shell of the ion as well as dehydration of the lipid membrane. The latter is supported by DSC measurements suggesting that the binding leads to a tighter packing of the lipids. The endothermic reaction enthalpies increase in absolute value with decreasing the size of the bare cation following the Hofmeister series. The ITC data also suggest that binding continues for all alkali cations even beyond molar stoichiometry of the bulk concentrations. At the same time,

(49) Koynova, R.; Caffrey, M. *Biochim. Biophys. Acta* **1998**, *1376*, 91–145.
(50) http://avantilipids.com/.
(51) Heimburg, T. *Biochim. Biophys. Acta* **1998**, *1415*, 147–162.

(52) Riske, K. A.; Amaral, L. Q.; Lamy, M. T. *Langmuir* **2009**, *25*, 10083–10091.
(53) Heimburg, T. *Biophys. J.* **2000**, *78*, 1154–1165.

the electrophoretic mobility measurements suggest that binding of lithium ions is observed well beyond the point of electrostatic charge compensation. This behavior is easily explained by considering the ion–membrane interaction as a "binding-by-dehydration" process.

Supporting Information Available: Data on the integrated heats of dilution and binding titrations corresponding to the heat flow data in Figure 3. This material is available free of charge via the Internet at http://pubs.acs.org.